

Bose-Glass and Fermi-Glass

Korekiyo Takahashi (✉ korekiyo@gmail.com)

Hokkaido University

Satoshi Tanda

Hokkaido University

Hideaki Obuse

Hokkaido University

Keiji Nakatsugawa

National Institute for Material Science

Masahito Sakoda

Hokkaido university <https://orcid.org/0000-0001-7134-2380>

Yoshiko Nanao

University of St Andrews

Michio Naito

Tokyo University of Agriculture and Technology

Hiroyoshi Nobukane

Hokkaido University <https://orcid.org/0000-0002-5138-4601>

Physical Sciences - Article

Keywords:

Posted Date: April 5th, 2022

DOI: <https://doi.org/10.21203/rs.3.rs-1509383/v1>

License:  This work is licensed under a Creative Commons Attribution 4.0 International License.

[Read Full License](#)

Bose-Glass and Fermi-Glass

Korekiyo Takahashi^{1,2,7}, Keiji Nakatsugawa^{2,6}, Masahito Sakoda^{1,2}, Yoshiko Nanao³, Michio Naito⁴, Hiroyoshi Nobukane^{5,2}, Hideaki Obuse^{1,2}, Satoshi Tanda^{1,2}

¹*Department of Applied Physics, Hokkaido University, Sapporo, 060-8628, Japan*

²*Center of Education and Research for Topological Science and Technology,*

Hokkaido University, Sapporo, 060-8628, Japan

³*School of Physics and Astronomy,*

University of St. Andrews, Fife, KY16 9SS, Scotland

⁴*Department of Applied Physics, Tokyo University of
Agriculture and Technology, Tokyo, 184-8588, Japan*

⁵*Department of Physics, Hokkaido University, Sapporo, 060-0810, Japan*

⁶*International Center for Materials Nanoarchitectonics,
National Institute for Material Science, Tsukuba, 305-0044 Japan*

⁷*Nomura Research Institute, Ltd., Tokyo, 100-0004, Japan*

Abstract

It is known that two-dimensional superconducting materials undergo a quantum phase transition from a localized state to superconductivity. When the disordered samples are cooled, bosons (Cooper pairs) are generated from Fermi glass and reach superconductivity through Bose glass. However, there has been no *universal* expression representing the transition from Fermi glass to Bose glass.

Here, we discovered an experimental renormalization group flow from Fermi glass to Bose glass in terms of simple β -function analysis. To discuss the universality of this flow, we analyzed manifestly different systems, namely a Nd-based two-dimensional layered perovskite and an ultrathin Pb film. We find that all our experimental data for Fermi glass fall beautifully into the conventional self-consistent β -function. Surprisingly, however, flows vertical to the conventional β -function are observed in the weakly localized regime of both systems, where localization becomes even weaker. We show that the vertical flow is evidence for the existence of Bose glass. Consequently, we confirm a universal quantum transition from Bose glass to Fermi glass with the new two-dimensional critical sheet resistance close to $R_{\square} = h/e^2$.

I. INTRODUCTION

The electric conductance in the quantum localized regime (a regime where the electrical resistance increases as the temperature decreases) of two-dimensional (2D) disordered systems has been discussed in terms of Fermi glass¹⁻⁷, i.e., Mott localization^{8,9} for strong correlated systems and Anderson localization¹⁰⁻¹⁵ for non-interacting systems¹⁶, and Bose glass^{17,18}. The Bose-glass phase is an insulator phase with properties similar to those of Fermi glass, and can be described as the phase where the 2D bosons are localized as a result of the quenched 2D disorder. Anderson localization has been studied using β -function analysis^{10,19}. Mott localization has been studied via Mott variable range hopping conduction (VRH)²⁰ and via Fisher scaling for the boson Hubbard model^{8,21,22}. Recently, Kapitulnik *et al.*²³ have shown that there is an anomalous metal state that overturns the conventional wisdom in the regime below superconducting critical sheet resistance^{8,24} $h/4e^2$ and different from the quantum localized regime. However, a boson-fermion mixture or a transition from Fermi glass to Bose glass has not been considered in the quantum localized regime.

Here, we discover an experimental renormalization group flow from Fermi glass to Bose glass in terms of β -function analysis. To discuss the universality of this flow, we analyzed manifestly different systems, namely a Nd-based two-dimensional layered perovskite and an ultrathin Pb film. The layered perovskite structure of Nd_2CuO_4 and Nd_2PdO_4 is called a T' -structure²⁵, and it has an ideal 2D electron conductance because the conducting layer is composed of square planar units. Figure 1 shows the temperature dependence of the electric resistance for $\text{Nd}_2\text{CuO}_{4-x}\text{F}_x$ single crystals²⁶, $\text{Nd}_{2-x}\text{Ce}_x\text{CuO}_4$ thin films²⁷, and $\text{Nd}_{2-x}\text{Ce}_x\text{PdO}_4$ thin films²⁸. Doping causes a Nd_2CuO_4 system to undergo a quantum phase transition from the localized state to the superconducting state, i.e. superconductivity - insulating (S-I) transition. Superconductivity is not observed in a Nd_2PdO_4 system regardless of the doping amount²⁸. On the other hand, the ultrathin Pb film²⁹ is grown sequentially *in situ* by the evaporation of Pb. The film changes to a superconductor from an insulator as the film thickness increases (FIG. 1).

We find that all experimental data in Fermi glass fall beautifully into the conventional self-consistent β -function. Surprisingly, however, flows vertical to the conventional β -function were observed in the weakly localized regimes of both systems, where localization becomes even weaker. We show that the vertical flow is evidence for the existence of Bose glass by

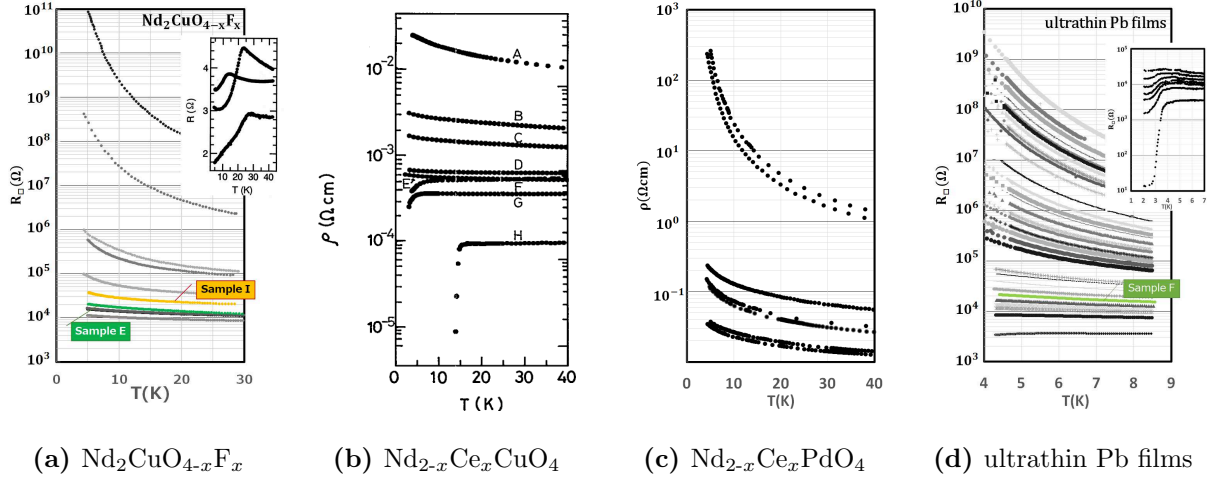


FIG. 1: The temperature dependence of the electric resistivity 1a (a) $\text{Nd}_2\text{CuO}_{4-x}\text{F}_x$ ²⁶, (b) $\text{Nd}_{2-x}\text{Ce}_x\text{CuO}_4$ ²⁷, (c) $\text{Nd}_{2-x}\text{Ce}_x\text{PdO}_4$ ²⁸ and (d) ultrathin Pb films²⁹ (thickness changed from 13.8Å to 42.8Å). Superconductivity-insulator transition is observed in (a) $\text{Nd}_2\text{CuO}_{4-x}\text{F}_x$ (the inset shows the superconducting state), $\text{Nd}_{2-x}\text{Ce}_x\text{CuO}_4$ and (d) ultrathin Pb films (the inset shows the superconducting state), while in (c) $\text{Nd}_{2-x}\text{Ce}_x\text{PdO}_4$ only the insulating state appears. Sample E of $\text{Nd}_2\text{CuO}_{4-x}\text{F}_x$, Sample I of $\text{Nd}_2\text{CuO}_{4-x}\text{F}_x$ and Sample F of ultrathin Pb films will be discussed in detail later. Sample E of $\text{Nd}_2\text{CuO}_{4-x}\text{F}_x$ is shown to be Bose glass and Sample I of $\text{Nd}_2\text{CuO}_{4-x}\text{F}_x$ is shown to be Fermi glass. Sample F of ultrathin Pb films show a change from Fermi glass to Bose glass as the temperature become lower.

using an experimental β -function and the temperature-derivative equation of the β -function (β' -function). Consequently we can confirm that there is a universal quantum transition from Bose glass to Fermi glass with the new two-dimensional critical sheet resistance close to $R_\square = h/e^2$. Since the Bose-glass phase in two types of Nd-based two-dimensional layered perovskites and Pb ultrathin films both exhibit a β' -function different from that of the Fermi-glass phase, with R_\square between h/e^2 and $h/4e^2$, this phenomenon is considered universal.

II. β -FUNCTION ANALYSIS

We investigate our experimental results with β -function analysis^{10,13}, which is applicable from weak to strong localization regimes. The β -function is defined as $\beta(g) \equiv d \ln g / d \ln L$, where L is the sample size and g is the dimensionless conductance [$g = (\hbar/e^2)\sigma$]. The

β -function shows the flow of electronic states as a function of size L , and can be used to determine whether it is delocalized or localized, and even weakly or strongly localized. With orthogonal class in 2D systems, $\beta(g) < 0$ means that the system always belongs to the localized phase due to Anderson localization regardless of the size L , but this is not the case for systems with a strong spin-orbit interaction, or for the quantum Hall effect. In such cases, the form of the β -function changes depending on the state of localization. In other words, if we view the form of the β -function as a renormalization group flow, we can understand the universality of the electronic state with the scale transformation.

Experimentally, L is taken to be the cutoff length due to inelastic scattering: $L^2 = DT^{-p}$. D is the diffusion constant, and T is temperature. The value of exponent p depends on the inelastic scattering mechanism. For Nd-based 2D layered perovskite systems, $p = 1.0$ ²⁶, for ultrathin Pb films, $p = 2.1$ ²⁹. So, the β -function is derived from the experimental data of the temperature dependence of the conductance as follows:

$$\beta_{\text{EXP.}}(g) = -\frac{2}{p} \frac{d \ln g}{d \ln T}. \quad (1)$$

This equation is predicted to behave as follows from weak to strong localized regimes; With a weakly localized regime, namely the 2D Anderson localization theory with conductance $\sigma = \sigma_0 + \sigma_1 \ln T$, we obtain the simple relation,

$$\beta_{\text{EXP.}}(g) = -\frac{2}{p} \frac{d \ln(\sigma_0 + \sigma_1 \ln T)}{d \ln T} = -\frac{2}{p} \frac{\sigma_1}{\sigma} = -\frac{1}{\pi^2 g} \sim -1/g. \quad (2)$$

Since σ_1 contains p , the result of the calculation is that p cancels out and $\beta_{\text{EXP.}}(g)$ is related only to g . With a strong localized regime, namely the VRH theory in Mott 2D, $g \propto \exp(-\varepsilon_{\text{VRH}}/T^{1/3})$, so that, $\beta_{\text{EXP.}}(g) \sim \ln g$. This ε_{VRH} is equal to the generalized activation energy³⁰.

On the other hand, in the self-consistent theory of the β -function, Vollhardt and Wölfle gave a single 2D system conductivity formula for orthogonal classes from weakly to strongly localized regimes^{31,32}.

$$g_{\text{VW}}(x) = \frac{1}{2\pi^2} (x+1) \ln \left(\frac{1}{x^2} + 1 \right) \exp(-x), \quad (3)$$

Here, $x = L/\xi \propto T^{-p/2}/\xi$, ξ is the localization length. Furthermore, the β -function from

eq.(3) can be calculated as follows,

$$\beta_{\text{vw}}(g) = \frac{d \ln g_{\text{vw}}(x)}{d \ln x} = - \left(\frac{x^2}{x+1} + \frac{2}{(x^2+1) \ln \left(\frac{1}{x^2} + 1 \right)} \right). \quad (4)$$

We analyzed our experimental data by using the above equations: first we estimated ξ from eq.(3), next we described the β -function obtained from eq.(4), finally we overlaid the $\beta_{\text{EXP.}}(g)$ data of eq.(1) and the $\beta_{\text{vw}}(g)$ data of eq.(4), to verify whether or not they matched. We see that all the data from weakly to strongly localized regimes fall into $\beta_{\text{vw}}(g)$ (Inset of FIG. 2). However, if we take a closer look at the weakly localized regime, as shown in FIG. 2, we discover that the data exhibit different *vertical flows* (indicated by the red arrows) against the usual Anderson localization β -function curve (indicated by the blue arrows). In the weakly localized regime, these vertical flows are present in both Nd-based 2D layered perovskite and ultrathin Pb films. In some ultrathin Pb film samples, it is clear that the flow changes from the usual Anderson localization flow to the vertical flow at a certain temperature (e.g., Pb-sample-F surrounded by a dotted circle).

III. VERTICAL FLOWS AND BOSE GLASS

To understand the mechanism of vertical flows, we analyze the temperature dependence of resistivity greater detail again. The functional forms of these vertical flows appear in the weakly localized regime, but are not adapted to $-1/g$. Therefore, we analyzed two samples before and after the vertical flow occurred; namely (a) $\text{Nd}_2\text{CuO}_{4-x}\text{F}_x$ (NCOF) sample E in which this vertical flow appears and (b) NCOF sample I in which the vertical flow does not appear. As a result, we find a difference in the temperature dependence of conductivity and resistivity. As shown in FIG. 3, the $\ln T$ dependence of the NCOF-sample-E resistivity is more suitable than that of the conductivity, whereas the NCOF-sample-I conductivity has $\ln T$ dependence according to the Anderson localization theory. Although these are in the same weakly localized regime, the vertical flow is clearly characterized by $\rho \sim \ln(1/T)$ rather than by $\sigma \sim \ln T$. Das *et al.*³³ pointed out that the weak localization of bosons occurring on the insulator side of the S-I transition in 2D is characterized by $\rho \sim \ln(1/T)$. Therefore, the state of the sample with the vertical flow can be regarded as boson localization, or the Bose-glass phase. These experimental results indicate that the Bose glass regime has been

found.

IV. TRANSITION FROM BOSE GLASS TO FERMI GLASS

Next, to investigate the condition of the change from Bose glass to Fermi glass, we plotted the temperature dependence of $\beta_{\text{EXP.}}(g)$ instead of the resistance as shown in FIG. 4 with a series of experimental data. Interestingly, the temperature dependence of $\beta_{\text{EXP.}}(g)$ in the weakly localized regime is very similar to the S-I transition graph. As the localization of each sample weakens (from the bottom to the top of FIG. 4), the slope of each set of data changes continuously from positive to negative in both Nd-based 2D layered perovskite and ultrathin Pb films. To understand the change in the slope of $\beta_{\text{EXP.}}(g)$ flows in FIG. 4, we use the temperature-derivative equation of the β -function shown below,

$$\beta'_{\text{EXP.}}(g) = -\frac{d \ln |\beta_{\text{EXP.}}(g)|}{d \ln T}. \quad (5)$$

The change in the β -function flow should appear in the positive or negative sign of $\beta'_{\text{EXP.}}(g)$. Substituting the two equations $\sigma = \sigma_0 + \sigma_1 \ln T$ and $\sigma = 1/\rho = 1/(\rho_0 + \rho_1 \ln(1/T))$ ($\sigma, \sigma_0, \sigma_1, \rho_0, \rho_1 > 0$) we see that the signs are different as follows.

$$\beta'_{\text{EXP.}}(g) \simeq \frac{\sigma_1}{\sigma_0 + \sigma_1 \ln T} > 0, (\sigma = \sigma_0 + \sigma_1 \ln T) \quad (6)$$

$$\beta'_{\text{EXP.}}(g) \simeq -\frac{\rho_1}{\rho_0 + \rho_1 \ln(1/T)} < 0, (\sigma = \frac{1}{\rho} = \frac{1}{\rho_0 + \rho_1 \ln(1/T)}). \quad (7)$$

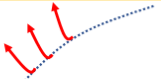
These calculation results confirm that the slope of $\beta_{\text{EXP.}}(g)$ reflects the temperature-dependent functional form of the conductivity and resistivity. To check this, we analyzed all the data for $\beta'_{\text{EXP.}}(g) < 0$ and found that they were more suitable for $\rho \sim \ln(1/T)$ than $\sigma \sim \ln T$. However, in the ultrathin Pb film data in FIG. 4 (b), there were samples where the sign of $\beta'_{\text{EXP.}}(g)$ changed from positive to negative when the temperature decreased. For Pb-sample-F, the sign of $\beta'_{\text{EXP.}}(g)$ changed around 6K. Since the superconducting transition temperature T_c of Pb (in the clean system) is around 7.2K, it is conceivable that bosons are formed. On the other hand, NCOF-sample-E did not exhibit any change of sign. This may be attributed to the measurement temperature range. Another set of data measured up to the high temperature regime was analyzed, and the change was confirmed below the superconducting transition temperature T_c of the $\text{Nd}_2\text{Pd}_{1-x}\text{Cu}_x\text{O}_{4-y}\text{F}_y$ (See Appendix A).

We also investigated the critical value of $\beta_{\text{EXP.}}(g)$, denoted as β_C , when the slope of $\beta'_{\text{EXP.}}(g)$ went to zero. From FIG. 4, β_C was obtained by using the slope and the intercept of the vertical axis for each sample at a specific low temperature. We obtained $\beta_C = -0.6 \pm 0.1$ with these two different types of samples (see Appendix B). This value is almost equal to $-0.64 (\simeq -2/\pi)$ and becomes the value of $g = 1/2\pi$, which we can convert to $\beta = -2/\pi$ by using eq.(2). The critical g does not indicate $R_{\square} = h/4e^2$ of the superconducting critical sheet resistance, but is at least close to $R_{\square} = h/e^2$ of the critical sheet fermion resistance. Mapping these values in FIG. 2 as a yellow star, we can see that the phenomenon of these vertical flows occurs at least when g is larger than $1/2\pi$. This $g = 1/2\pi$ value is transformed into the dimensionless version of the critical sheet fermion resistance $R_{\square} = h/e^2$. Based on the above results, at least two conditions are required to generate Bose-glass; $\beta'_{\text{EXP.}}(g) < 0$ and $R_{\square} < h/e^2$. The point at which the sign of $\beta'_{\text{EXP.}}(g)$ changes is related to the superconducting transition temperature T_c . This experimental analysis as regards the β -function clearly demonstrated the criteria for the Fermi-glass to Bose-glass transition. In other words, it proved the existence of boson formation even in a localized regime.

V. DISCUSSION AND CONCLUSION

We suggest that the fermion-only theory may be insufficient to explain the weakly localized regime just before reaching superconductivity in *2D disordered* superconducting materials. Fisher's theory is also insufficient because it is based on boson-only or fermion-only in the strongly localized regime represented by VRH. So, the boson-fermion mixture state and boson-only state in the weakly localized regime are an important area in clarifying the relationship between statistics (fermion, boson, and anyon) and localization. We discover an experimental renormalization group flow from Fermi glass to Bose glass by employing β -function analysis. To discuss the universality of Bose-glass flow, we analyzed distinctively different systems, namely a Nd-based two-dimensional layered perovskite and an ultrathin Pb film. What these two systems have in common is that they are both 2D disordered systems, but the difference is that a Nd-based 2D layered perovskite is disordered by doping while an ultrathin Pb film is structurally disordered. Furthermore, unlike an ultrathin Pb film, a Nd-based 2D layered perovskite is a strongly correlated electron system⁹. Although these two systems may have different superconductivity mechanisms, the flow of the

TABLE I: This table summarizes the experimental results. In the weakly localized regime where 2D Anderson localization dominates, both Fermi-glass and Bose-glass exist. The existence of the Bose-glass regime is clearly shown by the experimental β -function and the sign of the β' -function (the temperature derivative of the experimental β -function). We confirm a universal quantum transition from Bose glass to Fermi glass with the new two-dimensional critical sheet resistance close to $R_{\square} = h/e^2$ at $\beta' = 0$.

Weakly localized regime			
	Function	β	β'
Fermi-Glass	$\sigma = \sigma_0 + \sigma_1 \ln T$		+
Bose-Glass	$\rho = \rho_0 + \rho_1 \ln(1/T)$		-

$\sim \frac{h}{e^2}$ (at $\beta' = 0$)

experimental β -function exhibits the same behavior.

The analysis results obtained for the two systems in common are shown in TABLE I. These results suggest the following mechanism of universal quantum transition. With varying disorder in the weakly localized regime, Anderson localization ($\sigma \sim \ln T$) is observed when R_{\square} is larger than h/e^2 . When R_{\square} is smaller than h/e^2 , bosons and vortices are generated and the state becomes Bose glass. Furthermore, when R_{\square} is smaller than $h/4e^2$, fermions disappear and superconductivity occurs. It seems reasonable that Bose glass appears between h/e^2 and $h/4e^2$.

Paalanen *et.al.*¹⁸ identified Bose glass as the regime where the Hall resistance ρ_{xy} has a zero or a finite value when the longitudinal resistance ρ_{xx} diverges at low temperatures and in a certain magnetic field. On the other hand, we used the experimental β -function to identify the flow vertical to the 2D Anderson localized flow as Bose glass. This analysis constitutes a simple method of identifying weak boson/fermion localization. The results of Paalanen *et al.*'s experiment and ours are summarized in the phase diagram shown in FIG. 5. As an application of these results, even if superconductivity does not appear in a 2D material, the discovery of Bose glass flow in its β -function may provide a hint that could allow us to make the material superconductive by changing the disorder parameters.

VI. ACKNOWLEDGEMENTS

We are grateful to K. Yakubo, K. Ichimura and T. Matsuyama for suggesting the topic dealt with in this paper. We also thank many of those who attended the Forum of Localisation 2020. We have gained useful insights. Finally, we would like to thank S. Ozeki, K. Kagawa and K. Inagaki who studied together about 30 years ago, and T. Nakayama for introducing such a wonderful physics field.

-
- ¹ Anderson, P. W. The Fermi Glass: Theory and Experiment, 353–359.
- ² Fleishman, L. & Anderson, P. W. Interactions and the anderson transition. Phys. Rev. B **21**, 2366–2377 (1980).
- ³ Freedman, R. & Hertz, J. A. Theory of a fermi glass. Phys. Rev. B **15**, 2384–2398 (1977).
- ⁴ Abrahams, E., Kravchenko, S. V. & Sarachik, M. P. Metallic behavior and related phenomena in two dimensions. Rev. Mod. Phys. **73**, 251–266 (2001).
- ⁵ Spivak, B., Kravchenko, S. V., Kivelson, S. A. & Gao, X. P. A. Colloquium: Transport in strongly correlated two dimensional electron fluids. Rev. Mod. Phys. **82**, 1743–1766 (2010).
- ⁶ Popović, D., Fowler, A. B. & Washburn, S. Metal-insulator transition in two dimensions: Effects of disorder and magnetic field. Phys. Rev. Lett. **79**, 1543–1546 (1997).
- ⁷ Bogdanovich, S. c. v. & Popović, D. Onset of glassy dynamics in a two-dimensional electron system in silicon. Phys. Rev. Lett. **88**, 236401 (2002).
- ⁸ Fisher, M. P. A., Grinstein, G. & Girvin, S. M. Presence of quantum diffusion in two dimensions: Universal resistance at the superconductor-insulator transition. Phys. Rev. Lett. **64**, 587–590 (1990).
- ⁹ Imada, M., Fujimori, A. & Tokura, Y. Metal-insulator transitions. Rev. Mod. Phys. **70**, 1039–1263 (1998).
- ¹⁰ Abrahams, E., Anderson, P. W., Licciardello, D. C. & Ramakrishnan, T. V. Scaling theory of localization: Absence of quantum diffusion in two dimensions. Phys. Rev. Lett. **42**, 673–676 (1979).
- ¹¹ Abrahams, E. 50 Years of Anderson Localization (World Scientific, 2010).
- ¹² Anderson, P. W. Four last conjectures (2018). arXiv:1804.11186.

- ¹³ Lee, P. A. & Ramakrishnan, T. V. Disordered electronic systems. Rev. Mod. Phys. **57**, 287–337 (1985).
- ¹⁴ Evers, F. & Mirlin, A. D. Anderson transitions. Rev. Mod. Phys. **80**, 1355–1417 (2008).
- ¹⁵ Obuse, H., Subramaniam, A. R., Furusaki, A., Gruzberg, I. A. & Ludwig, A. W. W. Conformal invariance, multifractality, and finite-size scaling at anderson localization transitions in two dimensions. Phys. Rev. B **82**, 035309 (2010).
- ¹⁶ Gruzberg, I. A., Read, N. & Vishveshwara, S. Localization in disordered superconducting wires with broken spin-rotation symmetry. Phys. Rev. B **71**, 245124 (2005).
- ¹⁷ Fisher, M. P. A., Weichman, P. B., Grinstein, G. & Fisher, D. S. Boson localization and the superfluid-insulator transition. Phys. Rev. B **40**, 546–570 (1989).
- ¹⁸ Paalanen, M. A., Hebard, A. F. & Ruel, R. R. Low-temperature insulating phases of uniformly disordered two-dimensional superconductors. Phys. Rev. Lett. **69**, 1604–1607 (1992).
- ¹⁹ Evers, F. & Mirlin, A. D. Anderson transitions. Rev. Mod. Phys. **80**, 1355–1417 (2008).
- ²⁰ F.Mott, N. Conduction in non-crystalline materials. The Philosophical Magazine: A Journal of Theoretical Experimental and Applied Physics **19**, 835–852 (1969).
- ²¹ Fisher, M. P. A. Quantum phase transitions in disordered two-dimensional superconductors. Phys. Rev. Lett. **65**, 923–926 (1990).
- ²² Haldar, P., Laad, M. S. & Hassan, S. R. Quantum critical transport at a continuous metal-insulator transition. Phys. Rev. B **94**, 081115 (2016).
- ²³ Kapitulnik, A., Kivelson, S. A. & Spivak, B. Colloquium: Anomalous metals: Failed superconductors. Rev. Mod. Phys. **91**, 011002 (2019).
- ²⁴ Haviland, D. B., Liu, Y. & Goldman, A. M. Onset of superconductivity in the two-dimensional limit. Phys. Rev. Lett. **62**, 2180–2183 (1989).
- ²⁵ Müller-Buschbaum, H. & Wollschläger, M. Über ternäre oxocuprate. vii. zur kristallstruktur von Nd_2CuO_4 . Zeitschrift für anorganische und allgemeine Chemie **414**, 76–80 (1975).
- ²⁶ Tanda, S., Takahashi, K. & Nakayama, T. Scaling behavior of the conductivity of $\text{Nd}_2\text{CuO}_{4-x-\delta}\text{F}_x$ single crystals: Evidence for orthogonal symmetry. Phys. Rev. B **49**, 9260–9263 (1994).
- ²⁷ Tanda, S., Honma, M. & Nakayama, T. Critical sheet resistance observed in high- T_c oxide-superconductor $\text{Nd}_{2-x}\text{Ce}_x\text{CuO}_4$ thin films. Phys. Rev. B **43**, 8725–8728 (1991).

- ²⁸ Nanao, Y. *et al.* Crystal growth and metal-insulator transition in two-dimensional layered rare-earth palladates. Phys. Rev. Materials **2**, 085003 (2018).
- ²⁹ Kagawa, K., Inagaki, K. & Tanda, S. Superconductor-insulator transition in ultrathin Pb films: Localization and superconducting coherence. Phys. Rev. B **53**, R2979–R2982 (1996).
- ³⁰ Hill, R. M. On the observation of variable range hopping. physica status solidi (a) **35**, K29–K34 (1976).
- ³¹ Vollhardt, D. & Wölfle, P. Scaling equations from a self-consistent theory of anderson localization. Phys. Rev. Lett. **48**, 699–702 (1982).
- ³² Wölfle, P. & Vollhardt, D. SELF-CONSISTENT THEORY OF ANDERSON LOCALIZATION: GENERAL FORMALISM AND APPLICATIONS, 43–71 (World Scientific, 2010).
- ³³ Das, D. & Doniach, S. Weakly localized bosons. Phys. Rev. B **57**, 14440–14443 (1998).

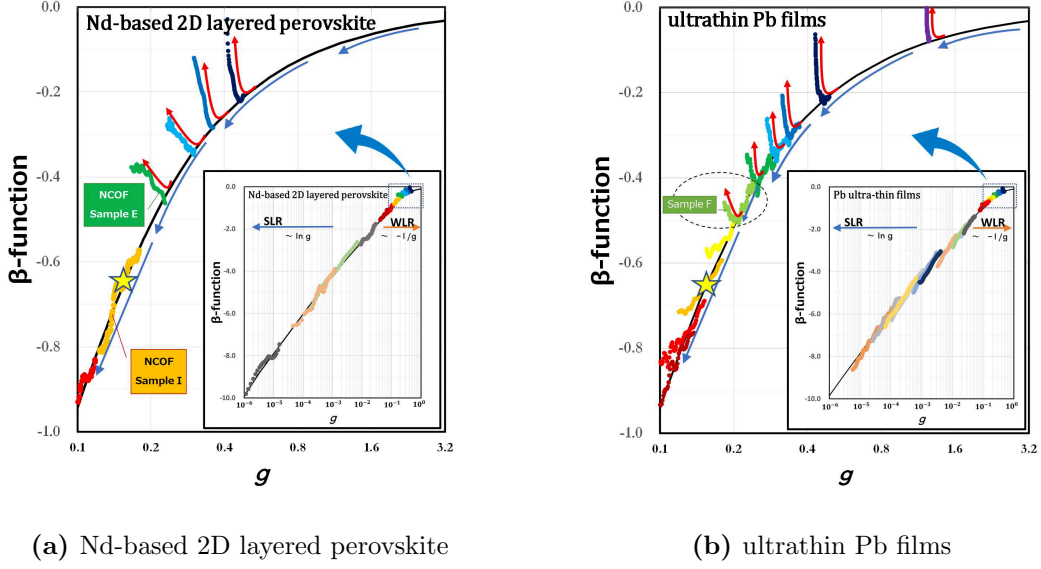
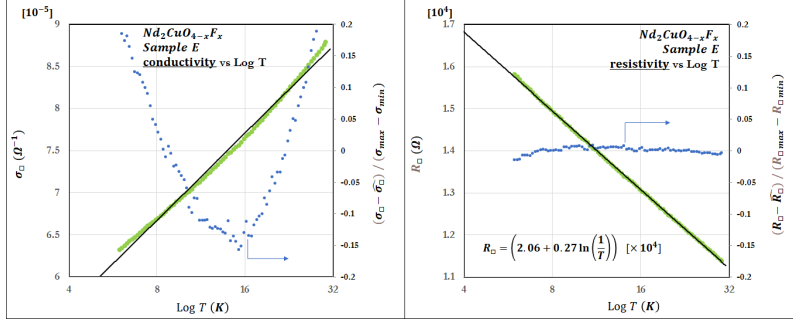
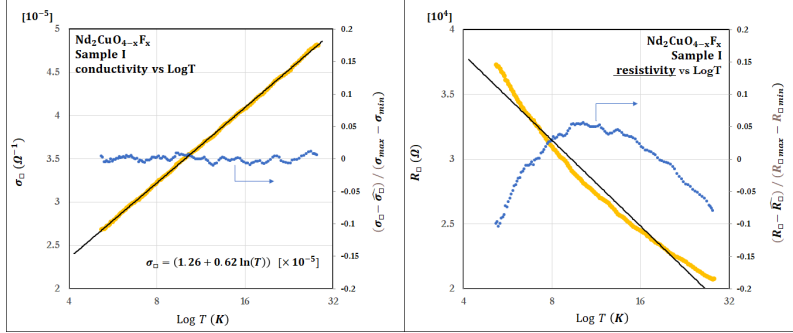


FIG. 2: Enlarged view of $\beta_{\text{EXP.}}(g)$ - the experimental β -function in a weakly localized regime. The inset shows $\beta_{\text{EXP.}}(g)$ from a weak to a strong localized regime. The black solid line shows $\beta_{\text{VW}}(g)$ — Vollhardt and Wölfle β -function (eq.(4)). The data for Nd-based 2D layered perovskite were plotted using resistance values from 5K to 25K. The data for ultrathin Pb films were plotted using resistance values from 4K to 10K. The color depends on the sample. If we view the β -function as a renormalization group flow, the Anderson localization β -function flow should behave like $\beta_{\text{VW}}(g)$ as indicated with the blue arrows. But, as shown by the red arrows, we discover a different flow which is vertical to $\beta_{\text{VW}}(g)$. In the weakly localized regime, these flows are present in both Nd-based 2D layered perovskite and ultrathin Pb films. In some ultrathin Pb film samples (e.g., Pb sample F surrounded by a dotted circle), it is clear that the flow changed from the usual Anderson localization flow to a vertical flow at a certain temperature. $\text{Nd}_2\text{CuO}_{4-x}\text{F}_x$ single crystals and $\text{Nd}_{2-x}\text{Ce}_x\text{CuO}_4$ thin films have different vertical flows, but $\text{Nd}_{2-x}\text{Ce}_x\text{PdO}_4$ does not have them. It is considered to be a phenomenon that is a precursor to the transition from weak localization to superconductivity. The yellow star in each graph indicates $g = 1/2\pi$ and $\beta = -2/\pi$, which is the dimensionless version of the critical sheet fermion resistance $R_{\square} = h/e^2$. This star is the boundary value at which the vertical flow occurs, as determined from FIG. 4 and Appendix B. Therefore, it proves that the phenomenon of these vertical flows is at its least apparent when R_{\square} is smaller than h/e^2 .

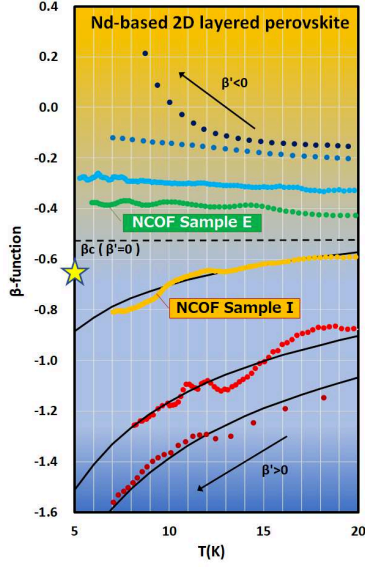


(a) $\text{Nd}_2\text{CuO}_{4-x}\text{F}_x$ Sample E in Bose-glass regime

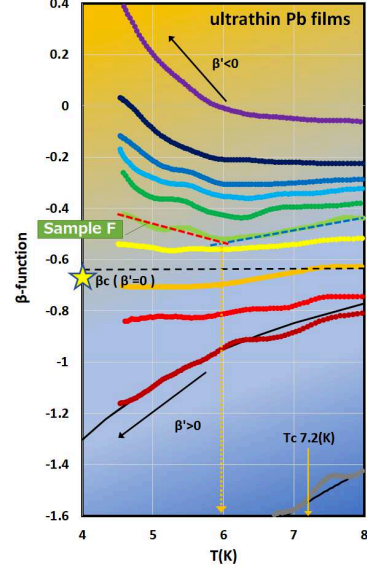


(b) $\text{Nd}_2\text{CuO}_{4-x}\text{F}_x$ Sample I in Fermi-glass regime

FIG. 3: Graphs comparing the $\log T$ dependence of σ_{\square} (left) and R_{\square} (right). We analyzed two samples before and after the vertical flow occurred; namely (a) $\text{Nd}_2\text{CuO}_{4-x}\text{F}_x$ (NCOF) sample E in which this vertical flow appears and (b) NCOF sample I in which the vertical flow does not appear. (NCOF-sample-E is along the red arrow and NCOF-sample-I is along the blue arrow in FIG. 2). The black solid line shows the regression line. The left vertical axis of the graph is σ_{\square} or R_{\square} . The horizontal axis of the graph is $\log T$, and the right vertical axis is the value obtained by subtracting $\hat{\sigma}_{\square}$ or \hat{R}_{\square} from the experimental value. For standardization, we divide by the value obtained by subtracting the minimum value from the maximum value of the experimental data on the vertical axis. Clearly, NCOF-sample-E is more suitable for the $\log T$ dependence of the resistivity than that of the conductivity, while NCOF-sample-I is the opposite. The vertical flow in the β -function indicates $\rho \sim \ln(1/T)$ rather than $\sigma \sim \ln T$. As a result, we find a difference between the $\log T$ dependence of the conductivity and resistivity.



(a) Nd-based 2D layered perovskite



(b) ultrathin Pb films

FIG. 4: Graphs of the relationship between the value of $\beta_{\text{EXP.}}(g)$ and temperature T with a series of the experimental data in a weakly localized regime. Interestingly, the temperature dependence of $\beta_{\text{EXP.}}(g)$ is very similar to the S-I transition graph. As the localization of each sample weakens (from the bottom to the top of the graph), the slope of each set of data changes continuously from positive to negative in both Nd-based 2D layered perovskite and ultrathin Pb films. The color depends on the sample. The black solid line shows $\beta_{\text{VW}}(g)$ — Vollhardt and Wölfle β -function (eq.(4)). We can see that among the weakly localized samples, those with strong localization ($\beta'_{\text{EXP.}}(g) > 0$) fit into $\beta_{\text{VW}}(g)$. However, in the (b) graph, as the localization becomes weaker, the slope of Pb sample F changes from positive (blue dotted line) to negative (red dotted line) when the temperature falls below around 6K. Since the superconducting transition temperature T_c of Pb (in a clean system) is around 7.2K, it is conceivable that boson appears. We also investigated the critical value of $\beta_{\text{EXP.}}(g)$, denoted as β_c when the slope of $\beta'_{\text{EXP.}}(g)$ goes to zero. β_c was obtained by using the slope and the intercept of the vertical axis for each sample at a specific low temperature. We obtained $\beta_c = -0.6 \pm 0.1$ in these two different types of samples. This value is almost the same $0.64 (\simeq 2/\pi)$ as shown by yellow star, and has a value of $g = 1/2\pi$ when converted using eq.(2). This value is the dimensionless version of the critical sheet fermion resistance $R_{\square} = h/e^2$.

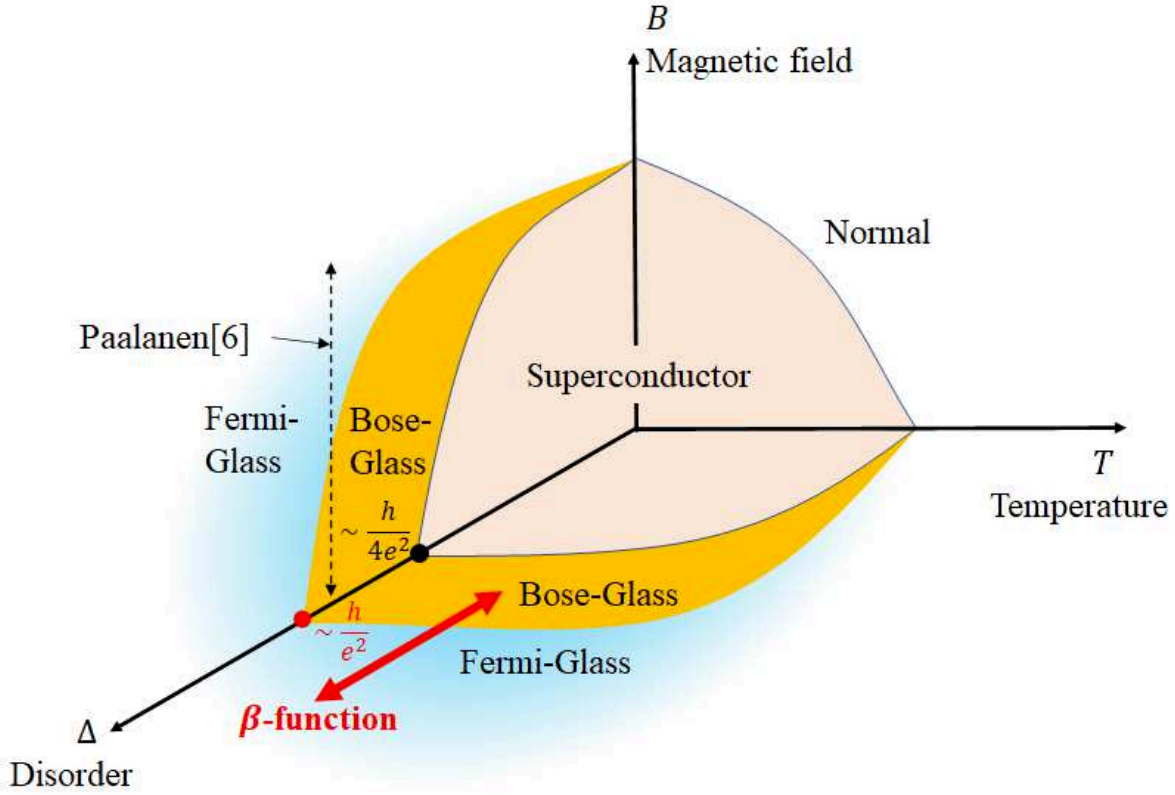


FIG. 5: Schematic phase diagram for 2D disordered superconducting materials. The analysis in this paper used the β -function to show the behavior of the change from Bose glass to Fermi glass before reaching superconductivity (bi-directional red arrow). The critical sheet resistance, which is the boundary between Bose glass and Fermi glass, is indicated to be around h/e^2 (red dot). The black dotted arrow represents Paalanen *et al.*'s experiments¹⁸.

Appendix A: $\beta_{\text{EXP.}}(g)$ and T with $\text{Nd}_2\text{Pd}_{1-x}\text{Cu}_x\text{O}_{4-y}\text{F}_y$

We analyze special substances which $\text{Nd}_2\text{Pd}_{1-x}\text{Cu}_x\text{O}_{4-y}\text{F}_y$ films grown on CaF_2 . The Nd-based high-temperature superconductor Nd_2CuO_4 develops superconductivity as a result of appropriate reduction treatment. We investigated the temperature dependence of the resistance of $\text{Nd}_2\text{Pd}_{1-x}\text{Cu}_x\text{O}_4$ in which this Cu was replaced with Pd (FIG. 6, left panel). If the proportion of Cu is large ($x = 0.84$), it is expected that bosons will be generated at a certain temperature and the $\beta_{\text{EXP.}}(g)$ slope will change. The analysis result is shown on the right in FIG. 6. At about 20K (red arrow) the experimental data moved away from $\beta_{\text{VW}}(g)$ and there was a positive and negative change in $\beta'_{\text{EXP.}}(g)$. This temperature is almost the same as the critical temperature T_c of the Nd-based high-temperature superconductor. FIG. 6 confirms the transition from Fermi-glass (yellow dots) to Bose-glass (green dots) on Nd-based 2D layered perovskite as well as ultrathin Pb films.

Appendix B: boundary value when $\beta'_{\text{EXP.}}(g) = 0$ is in the weakly localized regime

So, if there is a boundary between positive and negative $\beta'_{\text{EXP.}}(g)$ in the weakly localized regime, in short when $\beta'_{\text{EXP.}}(g) = 0$, what is the value of $\beta_{\text{EXP.}}(g)$ and the conductivity g ? For each graph in FIG. 4, we regarded $\beta_{\text{EXP.}}(g)$ as a linear function of T in a particular temperature range such as $\beta_{\text{EXP.}}(g) = aT + b$ (where a is the slope of $\beta_{\text{EXP.}}(g)$ and b is the intercept of $\beta_{\text{EXP.}}(g)$). FIG. 7 shows a graph in which a and b of each graph in FIG. 4 are mapped, and the $\beta_{\text{EXP.}}(g)$ value at $T = 0$ is obtained. From the experimental data in FIG. 7, we obtained $\beta_c = -0.6 \pm 0.1$ in these two different types of samples. This value is almost equal to $0.64 (= 2/\pi)$ and becomes the value of $g = 1/2\pi$ to which we can convert $\beta = -2/\pi$ using eq.(2). This g is a dimensionless version of the critical sheet fermion resistance $R_{\square} = h/e^2$. The boundary of $\beta'_{\text{EXP.}}(g) = 0$ separates the Bose-glass and Fermi-glass regimes. In other words, this result reveals that the condition for the occurrence of weakly localized $\rho \sim \ln(1/T)$ is $g > 1/2\pi$. This means that superconductivity cannot occur above $R_{\square} = h/e^2$, so the results of these analyses are consistent.

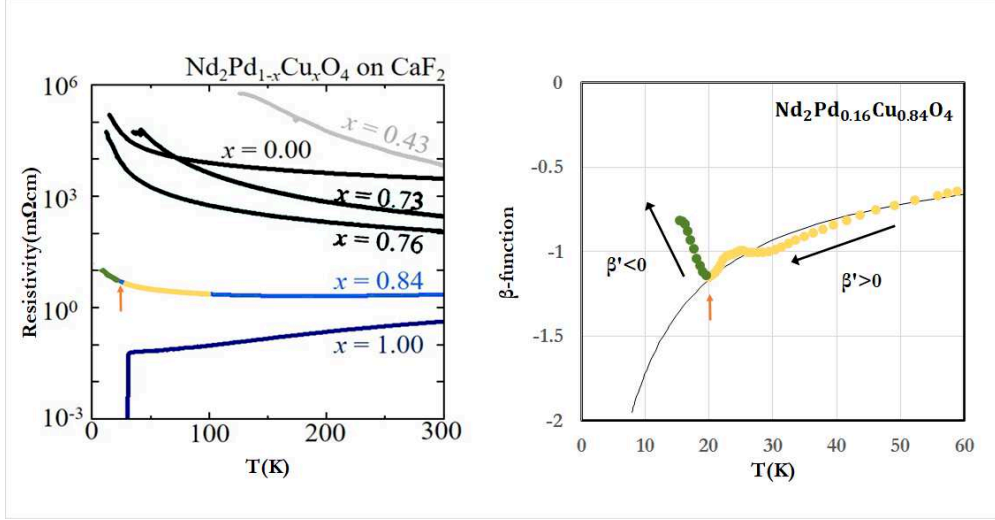
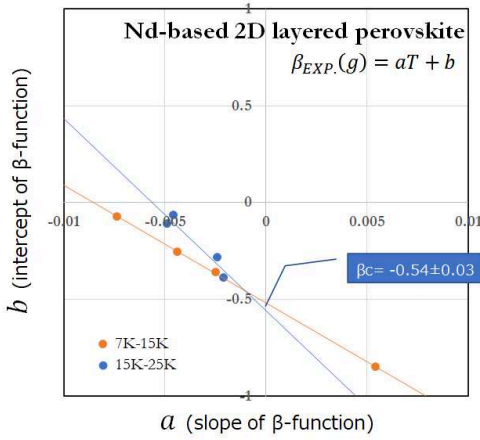
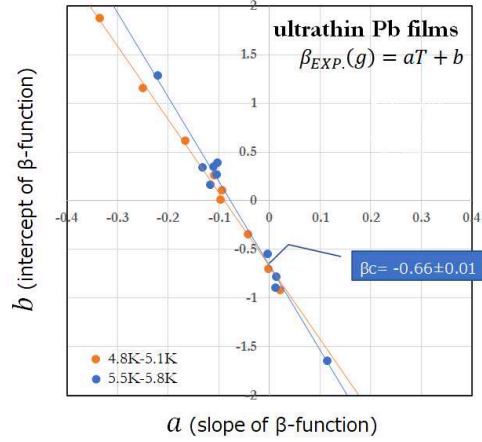


FIG. 6: The Left panel shows the temperature dependence of the resistance of $\text{Nd}_2\text{Pd}_{1-x}\text{Cu}_x\text{O}_{4-y}\text{F}_y$ films grown on CaF_2 ($x = 0.43 \sim 1.00$). The right panel shows the relationship between $\beta_{\text{EXP.}}(g)$ and temperature T with $\text{Nd}_2\text{Pd}_{0.16}\text{Cu}_{0.84}\text{O}_4$. Among the localized samples, this sample was the closest to the superconducting state. To calculate $\beta_{\text{EXP.}}(g)$ requires the dependence of the value of exponent p on the mechanism of inelastic scattering, but since it was not measured, it was calculated as $p = 1.5$. The black solid line shows $\beta_{\text{VW}}(g)$. It was at about 20K (red arrow) that the experimental data moved away from $\beta_{\text{VW}}(g)$ and the sign of $\beta'_{\text{EXP.}}(g)$ changed. This temperature is almost the same as the critical temperature T_c of the Nd-based high-temperature superconductor. No change in $\beta'_{\text{EXP.}}(g)$ was observed in samples other than $x = 0.84$. This graph confirms the transition from Fermi-glass (yellow dots) to Bose-glass (green dots) as the temperature is decreases.



(a) Nd-based 2D layered perovskite systems



(b) ultrathin Pb films

FIG. 7: The above graphs are the analysis to used to find a boundary value when $\beta'_{\text{EXP.}}(g) = 0$ in the weakly localized regime. For each graph in FIG. 4, we regarded $\beta_{\text{EXP.}}(g)$ as a linear function of T in a particular temperature range such as $\beta_{\text{EXP.}}(g) = aT + b$. The horizontal axis a is the slope of $\beta_{\text{EXP.}}(g)$ and the vertical axis b is the intercept of $\beta_{\text{EXP.}}(g)$. These graphs showed a and b of each graph in FIG. 4, and the $\beta_{\text{EXP.}}(g)$ value at $T = 0$ was obtained. From the experimental data obtained for the Nd-based 2D layered perovskite systems, we obtained $\beta_{\text{EXP.}}(g) = -0.54 \pm 0.03$. And from the experimental data for the ultrathin Pb films, we obtained $\beta_{\text{EXP.}}(g) = -0.66 \pm 0.01$. From the experimental data in FIG. 7, we obtained $\beta_C = -0.6 \pm 0.1$ in these two different types of samples. This value is almost equal to $0.64 (\simeq 2/\pi)$ and becomes a value of $g = 1/2\pi$, to which we can convert $\beta = -2/\pi$ using eq.(2). This g is the dimensionless version of the critical sheet fermion resistance $R_{\square} = h/e^2$. The boundary of $\beta'_{\text{EXP.}}(g) = 0$ separates the Bose-glass and Fermi-glass regimes.